Amorphous two-dimensional optical lattices with coherently controlled morphologies in quantum well structures

S. M. Sadeghi*
Photonami Inc., 50 Mural street, Richmond Hill, Ontario L4B 1E4, Canada
(Received 23 January 2005; revised manuscript received 11 June 2005; published 21 September 2005)

It is shown theoretically that the interface morphology of a quantum well structure and coherent control of its optical properties can be used to generate an amorphous two-dimensional optical lattice. This is done by considering the interaction of an *n*-doped double-quantum-well structure containing three conduction subbands with an infrared laser beam responsible for the generation of quantum interference in the transitions between these subbands. We show that when a well/barrier interface in this structure contains large-scale monolayer growth islands the lateral variation of the conduction subband energies changes the effects of quantum coherence in these transitions along the quantum well plane. In the presence of electron tunneling in the double-quantum-well structure this leads to lateral modulation of the complex susceptibilities of these transitions, allowing the infrared laser beam to coherently suppress or enhance refractive indices of these transitions in specific regions in this plane while they become transparent. In other regions, the same laser field generates large amount of gain or absorption with different refractive indices. It is shown that for a signal field propagating along the quantum well plane these processes can generate an amorphous optical lattice with a morphology determined by the roughness of the quantum well interfaces and the frequency and intensity of the infrared laser. In the absence of such an infrared laser this plane is transparent to the signal field and has a uniform refractive index.

DOI: 10.1103/PhysRevB.72.125336 PACS number(s): 78.67.De, 73.21.Fg, 68.55.Ac, 81.07.St

I. INTRODUCTION

Utilization of coherently controlled optical processes and light-matter interactions to spatially modulate refractive indices and absorption coefficients of atoms and solids has wide technological and fundamental application. This includes new avenues for active control of flow of light and manipulation of nonlinear optical processes in solids and atomic media by optimizing materials and geometric parameters of periodic structures. In a previous attempt off-resonant standing light wave was used to spatially modulate the resonances associated with electromagnetically induced transparency in an atomic medium.[1] Here the dynamic photonic band gap was used to convert a propagating light pulse into a stationary excitation. In another attempt excitons confined in a periodic quantum well structure was used to create an active photonic band gap using their super-radiant modes.[2,3] It has been shown that one can manipulate such a band gap using the ac Stark effect.[4] Moreover, in a recent study spatial modulation of the refractive index and absorption coefficient was predicted using resonant enhancement of the refractive index with vanishing absorption in the intersubband transitions in an *n*-doped quantum well (QW).[5] Here it was shown that by coherent reduction of absorption of a corrugated QW structure to zero while significantly enhancing its refractive index an active photonic band gap could be generated.

In this paper we propose a method that allows using coherently controlled optical processes in a QW structure and the well/barrier macroscopic interface roughness to spatially (laterally) modulate the complex susceptibilities associated with the conduction intersubband transitions. Using this method one can employ an intense infrared (ir) laser beam to make some regions in the plane of this structure transparent with coherently enhanced or suppressed refractive indices while other regions in this plane exhibit immense amount of gain or absorption with different refractive indices. This allows formation of an amorphous two-dimensional optical lattice for a specific wavelength of a signal (probe) field propagating along the QW plane. In the absence of the intense ir laser field, however, this plane is transparent to the signal field and has a uniform refractive index. We show that the morphology of such a lattice depends on the quantum well interfaces and can be dynamically controlled by changing the intensity and/or frequency of the intense ir laser field. This potentially allows one to coherently control propagation of the signal field in the QW plane. The optical lattices introduced in this paper have some similarities with those in atoms and multiple-quantum-well structures. In atomic systems a nearly resonant standing wave sets up a specific arrangement of atoms via ac Stark effect, allowing scattering of a signal field from transitions of bound atoms.[6,7] In a multiple-QW structure when the difference between the refractive indices of the wells and barriers is ignorable, the periodic modulation of the exciton susceptibilities is mainly responsible for the generation of the index and absorption contrasts.[2,3]

The optical lattices discussed in this paper are mainly based on two issues: (i) coherent optical processes caused by interaction of the intense ir laser field (control field) with a single *n*-doped double-QW structure, and (ii) impacts of the macroscopic interface fluctuations, i.e., large-scale monolayer (ML) growth islands, on these processes. In the presence of the signal field, the control field generates quantum interference in the conduction intersubband transitions, similar to that in the laser-induced transparency in atoms.[8] How-

ever, since the double-QW structure contains two adjacent wells separated by a thin barrier, electrons can tunnel from one subband to another. Therefore, as shown in this paper, by varying the frequency and/or intensity of the control field one can adjust the way such a process influences the quantum interference events, allowing us to resonantly enhance or suppress the refractive indices of the intersubband transitions while their absorption coefficients are coherently controlled.[9] Via variation of the intersubband transition energies along the QW plane, the role of the ML islands here is to laterally change the balance between the interference events and the effects caused by electron tunneling. This leads to lateral modulation of the interaction of the control field with the QW structure, changing the complex susceptibility associated with these transitions from one region of the QW plane to another. As shown in this paper, this causes a dynamic amorphous two-dimensional optical lattice.

The results presented in this paper can have dramatic applications in the design of optical devices and study of nonlinear optical processes in nanostructures. This is because of the fact that many passive and active optical devices such as waveguides, semiconductor optical amplifiers, and lasers, are index guided with certain amount of gain or absorption. Therefore, the lateral modulation of refractive index accompanied with the coherent control of absorption coefficient discussed in this paper can present further scope for the development of these devices and their monolithic integration. In addition, because of their wavelengths and polarizations, the results of this paper are particularly compatible with the infrared lasers such as quantum cascade and other intersubband-based lasers,[10] optical modulators, etc. They can also be used to envision an active photonic band gap using engineered interfaces.

II. INTERFACE MORPHOLOGY AND COHERENT CONTROL OF OPTICAL PROCESSES IN *n*-DOPED QUANTUM WELLS

It is well known that when the epitaxial growth process of a QW structure is interrupted for a period of time the atoms deposited on the surface diffuse, forming large smooth islands with one-monolayer steps.[11] The lateral dimension of these islands can become quite large (several micrometers) depending on the growth temperature and rate, interruption time and others.[12,13] A schematic representation of such morphology for an $Al_xGa_{1-x}As/GaAs/Al_xGa_{1-x}As$ QW structure is shown in Fig. 1. Here we assume that before deposition of the top $Al_xGa_{1-x}As$ layer the growth process was halted for a period of time, which is usually considered to be around 120 s.[14] As a result, the upper interface becomes relatively smooth but contains ±1 ML macroscopic thickness fluctuations (growth islands). Assuming that the GaAs layer was continuously grown on the lower $Al_xGa_{1-x}As$ barrier, as schematically shown in Fig. 1, the lower interface becomes relatively rougher (microscopic roughness) but contains no growth island. Such growth islands can split the interband photoluminescence spectrum of a QW into several peaks, causing ML splitting peaks.[15] They can also influence the intersubband transition energies, allowing an ir laser field to

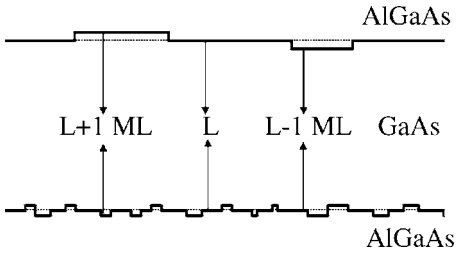

FIG. 1. Schematic illustration of microscopic and macroscopic fluctuations, respectively, at the lower and upper interfaces of an $Al_xGa_{1-x}As/GaAs/Al_xGa_{1-x}As$ QW structure. It is assumed that before deposition of the upper $Al_xGa_{1-x}As$ layer the growth process is interrupted for a period of time. *L* refers to the nominal width of the QW structure.

have different detunings from these transitions in different regions of the QW plane. Therefore, as shown in Ref. 16, when this field becomes intense it can influence the intersubband transitions in various parts of the QW plane differently. This leads to intersubband optical Stark shifts that can vary from one region to another, shifting some of the ML splitting peaks seen in the interband photoluminescence spectrum to lower frequencies while some others are pushed to higher frequencies.[16] The large growth islands can also be responsible for the inhomogeneous broadening of the intersubband transition linewidths,[17] and for the generation of distinct features in their absorption spectra.[18]

In this section we utilize these features to present a model that allows us to study spatial (lateral) modulation of absorption coefficients and refractive indices of the intersubband transitions in the plane of a QW structure. As mentioned in the Introduction, the key features of this model are (i) generation of quantum interference in the conduction intersubband transitions, (ii) incoherent pumping of one conduction subband by another, and (iii) the presence of interface growth islands. To accommodate these features here we adopt a semiconductor structure that contains a single *n*-doped double QW, as shown in Fig. 2. Nominally this structure contains 20-ML- and 10-ML-thick GaAs wells separated by 4 ML of $Ga_{0.58}Al_{0.42}As$ (middle barrier). The left and right barriers are the same as the middle barrier. We assume that the interface between the wider well (nominally

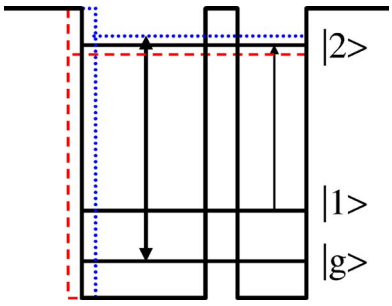

FIG. 2. (Color online) Schematic illustrations of the potential profiles of the double-QW structures in regions of the QW plane where the wider (left) QW thickness is 20 (solid line), 21 (dashed line), or 19 ML (dotted line). The two-sided arrow represents the control field and the one-sided arrow refers to the signal field.

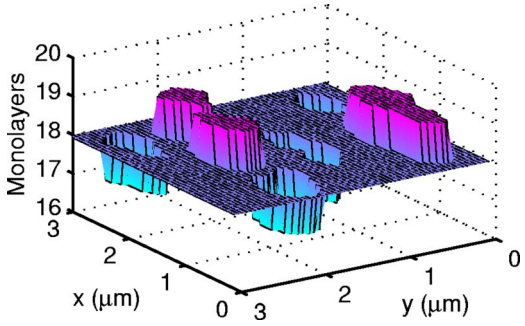

FIG. 3. (Color online) An oblique illustration of the interface between the left $Al_{0.42}Ga_{0.58}As$ barrier (top) and the nominally 20-ML-wide GaAs well (bottom). The terraces and valleys refer, respectively, to +1 and −1 ML fluctuations in the GaAs well thickness.

20 ML) and the left barrier contains large growth islands associated with ±1 ML thickness fluctuations of GaAs. In practice, this means that before the left barrier is grown, one needs to halt the growth process for an appropriate period of time (roughly 120 s) when deposition of the wider well over the middle barrier is completed. Figure 3 shows an oblique illustration of the morphology we assumed for the interface between these two layers. Here the valleys and terraces refer, respectively, to −1 and +1 ML changes in the thickness of the wider GaAs well. Note that since we assume the other layers of the structure are grown without any interruption, the interfaces of the 10-ML GaAs well and that between the middle barrier and the 20-ML well do not contain any island. Therefore, the overall effect of such a growth technique is generation of a double-QW structure where in some lateral regions the thickness of its wider GaAs well is either 19 ML (valleys) or 21 ML (terraces) while in the rest it is 20 ML (nominal thickness). The widths of the narrower GaAs well and the middle barrier remain unchanged all over the QW plane. In the following we refer to the double QW's in the valley and terrace regions as the 19-ML and 21-ML systems, respectively. The rest of the structure with the nominal specifications is called the 20-ML system. The potential profiles of these systems along the growth direction are schematically shown in Fig. 2 with dotted, dashed, and solid lines, respectively.

Note that in each of the three ML systems considered in Fig. 2 the lower transition level ($|1\rangle$) incoherently pumps the ground subband ($|g\rangle$) via electron tunneling. In addition, the upper transition level ($|2\rangle$) is coherently coupled to $|g\rangle$ by an intense laser (control field) while the signal field detects evolution of the 1-2 transition. These two fields are both polarized along the growth direction of the QW. The quantum interference in the systems shown in Fig. 2 happens between the 1-2 direct paths induced by the signal field and the indirect 1-2-g paths generated by both signal and control fields. Note also that it has been shown that when the g-1 transition energies are adjusted properly these systems can support gain in the 1-2 transitions[19] and even can be used for laser application.[20]

A full quantitative treatment of the interface morphology of the structure described above is complicated. It requires detailed information about the statistical features of the interfaces that not only change from one sample to another, but also from one part of a sample to the another. Here, in addition to the microscopic roughness, one should also consider lateral shapes of the islands, correlations between sizes and shapes of adjacent islands, etc.[21–23] In this paper, however, we are interested in the growth islands with scales much larger than Bohr radius. As discussed in Refs. 17 and 18, under such a condition and when the scale of growth islands are also larger than the QW width, one can treat the intersubband transitions within local approximation. Considering these issues and for the benefit of focusing on our objectives, we therefore treat the effects of the interface fluctuations in the interaction between the QW structure and the ir fields at a phenomenological level. Here to include the effects of energy relaxation of electrons from one island to another we adopt a model similar to that presented in Refs. 24–27. In these reports the lateral energy relaxation of excitons from higher-energy growth islands into regions with lower energies was studied within an average transport time approximation. In our model the lateral relaxation of electrons occurs when the control field is on. This is due to the fact that in the absence of this field the upper subbands are empty and the high carrier density (6×10^{11} cm^{-2}) screens the relatively small fluctuations of the first conduction subband energies.[17,18] We assume that the net average transport time of carriers from the 19-ML to 20-ML systems and from the 20-ML to 21-ML systems is around 50 ps (energy relaxation from the 19-ML to 21-ML systems is not included). This estimation is based on the overall dimension of the islands considered in this paper (around 1 μm) and the calculation of carrier transport time reported in Ref. 28 for a semiconductor layer with a flat potential.

Having these in mind, within the rotating-wave and effective-mass approximations we obtain the equation of motion of the density matrix of the QW system in the lth island, $\rho^{l,\mathbf{k}}$, as follows:

$$\frac{\partial\rho_{gg}^{l,\mathbf{k}}}{\partial t} = -i\Omega_c^l(\rho_{2g}^{l,\mathbf{k}} - \rho_{g2}^{l,\mathbf{k}}) + \Gamma_{2g}\rho_{22}^{l,\mathbf{k}} + r_t\rho_{11}^{l,\mathbf{k}} + \sum_{m=l-1,l+1}\lambda_{lm}^{\mathbf{k}}, \tag{1}$$

$$\frac{\partial\rho_{11}^{l,\mathbf{k}}}{\partial t} = -i\Omega_s^l(\rho_{12}^{l,\mathbf{k}} - \rho_{21}^{l,\mathbf{k}}) - r_t\rho_{11}^{l,\mathbf{k}} + \Gamma_{21}\rho_{22}^{l,\mathbf{k}} + \sum_{m=l-1,l+1}\lambda_{lm}^{\prime\mathbf{k}}, \tag{2}$$

$$\frac{\partial\rho_{22}^{l,\mathbf{k}}}{\partial t} = i\Omega_c^l(\rho_{2g}^{l,\mathbf{k}} - \rho_{g2}^{l,\mathbf{k}}) - i\Omega_s^l(\rho_{21}^{l,\mathbf{k}} - \rho_{12}^{l,\mathbf{k}}) - (\Gamma_{21} + \Gamma_{2g})\rho_{22}^{l,\mathbf{k}} - \lambda_{l,l+1}^{\prime\prime\mathbf{k}} + \lambda_{l,l-1}^{\prime\prime\mathbf{k}} - \sum_{m=l-1,l+1}(\lambda_{ml}^{\mathbf{k}} + \lambda_{ml}^{\prime\mathbf{k}}), \tag{3}$$

$$\frac{\partial\rho_{g2}^{l,\mathbf{k}}}{\partial t} = i[\Delta_c^{l,\mathrm{k}} + i\gamma_{g2}^{\mathrm{e\text{-}e}}(\mathrm{k}) + i\gamma_{g2}^{\mathrm{e\text{-}p}}]\rho_{g2}^{l,\mathbf{k}} + i\Omega_s^l\rho_{g1}^{l,\mathbf{k}} + i\Omega_c^l(\rho_{gg}^{l,\mathbf{k}} - \rho_{22}^{l,\mathbf{k}}), \tag{4}$$

$$\frac{d\rho_{1g}^{l,\mathbf{k}}}{dt} = -i[\delta_l^{\mathbf{k}} - i\gamma_{g1}^{e\text{-}e}(\mathrm{k}) - i\gamma_{1g}^{e\text{-}p}]\rho_{1g}^{l,\mathbf{k}} - i\Omega_s^l\rho_{2g}^{l,\mathbf{k}} + i\Omega_c^l\rho_{12}^{l,\mathbf{k}}, \tag{5}$$

$$\frac{\partial\rho_{12}^{l,\mathbf{k}}}{\partial t} = i[\Delta_s^{l,\mathrm{k}} - i\gamma_{12}^{e\text{-}p}]\rho_{12}^{l,\mathbf{k}} - i\Omega_s^l(\rho_{22}^{l,\mathbf{k}} - \rho_{11}^{l,\mathbf{k}}) - i\Omega_c^l\rho_{g1}^{l,\mathbf{k}}. \tag{6}$$

Here $\Omega_c^l = -\mu_{g2}^l E_c/\hbar$ and $\Omega_s^l = -\mu_{12}^l E_s/\hbar$ refer, respectively, to the Rabi frequencies of the control and signal fields with frequencies ω_c and ω_s and amplitudes E_c and E_s. μ_{g2}^l is the dipole moment associated with the g-2 transition and μ_{12}^l refers to that of the 1-2 transition in the lth island. For the 19, 20, or 21 ML system the former is found to be $1.0e$, $0.95e$, or $0.89e$ nm, respectively, while the latter is estimated to be $2.1e$, $2.0e$, or $1.96e$ nm (e is the electron charge). r_t is the rate of incoherent pumping of $|g\rangle$ caused by tunneling of electrons from $|1\rangle$. In Eqs. (4)–(6), $\Delta_c^{l,\mathbf{k}} = \omega_2^{l,\mathbf{k}} - \omega_g^{l,\mathbf{k}} - \omega_c$ and $\Delta_s^{l,\mathbf{k}} = \omega_2^{l,\mathbf{k}} - \omega_1^{l,\mathbf{k}} - \omega_s$ are the one-photon detunings of the control and signal fields, respectively, and $\delta_l^{\mathbf{k}} = \omega_1^{l,\mathbf{k}} - \omega_g^{l,\mathbf{k}} + \omega_s - \omega_c$ is the two-photon detuning. $\omega_j^{l,\mathbf{k}}$ refers to the frequency associated with the energy of an electron in the jth subband. $\gamma_{g1}^{e\text{-}e}(\mathbf{k})$ and $\gamma_{g2}^{e\text{-}e}(\mathbf{k})$ represent the electron-electron scattering effects in the dephasing rates of the g-1 and g-2 transitions. Although these rates are in general $\mathbf{k}$ dependent,[29] within the assumption of parabolic dispersions for the conduction subbands, we consider them in a phenomenological way equal to be 2 ps^{-1}. Note also that such a treatment bears the fact that in highly doped quantum well structures one can ignore nondiagonal dephasing rates (polarization scattering) in the intersubband transitions.[30,31] The electron-electron scattering in 1-2 transitions is also ignored, as the carrier densities in $|1\rangle$ and $|2\rangle$ are much less than that in $|g\rangle$, and electrons in these subbands are more dominantly influenced by electron–LO-phonon scattering processes. $\Gamma_{21} = 1/2$ ps^{-1} and $\Gamma_{2g} = 1/1.5$ ps^{-1} in Eqs. (1)–(3) refer, respectively, to the energy relaxation rates of electrons from $|2\rangle$ to $|1\rangle$ and from $|2\rangle$ to $|g\rangle$ caused by such scattering processes.[19,32] $\gamma_{ij}^{e\text{-}p}$ refer to the contributions of such processes to the intersubband transitions. The tunneling rate for electrons from $|1\rangle$ to $|g\rangle$ (r_t) is also taken to be 0.5 ps^{-1}. In general, this rate is strongly influenced by the energy spacing between these two subbands and the thickness of the middle barrier. For the structure considered in this paper (Fig. 2) the g-1 transition energy is around 95 meV, which is much larger than the LO phonon energy (36 meV). Therefore, the large phonon wave vector required for such a transition hampers the tunneling rate to some extent.[33]

$\lambda_{lm}^{\mathbf{k}}$ and $\lambda_{lm}^{\prime\mathbf{k}}$ in Eqs. (1) and (2) refer, respectively, to the effective pumping rates of $|g\rangle$ and $|1\rangle$ in the lth island (e.g., the 20-ML system) due to energy relaxation of electrons in $|2\rangle$ in the mth adjacent island (e.g., the 19- or 21-ML system). $\lambda_{l,l-1}^{\prime\prime\mathbf{k}}$ in Eq. (3), however, represents the pumping rate of $|2\rangle$ in the lth island by the electrons in $|2\rangle$ of an adjacent island with fewer ML's. Correspondingly, $\lambda_{ml}^{\mathbf{k}}$, $\lambda_{ml}^{\prime\mathbf{k}}$, and $\lambda_{l,l+1}^{\prime\prime\mathbf{k}}$ in Eq. (3) represent, respectively, decay of electrons from $|2\rangle$ in the lth island into $|g\rangle$, $|1\rangle$, and $|2\rangle$ of another island. These rates are associated with the average transport time of electrons from one island to another and are proportional to the electron densities in the $|2\rangle$'s of the donating islands. Here, however, since in each island $\lambda_{lm}^{\mathbf{k}}$ and $\lambda_{lm}^{\prime\mathbf{k}}$ [Eqs. (1) and (2)] are accompanied with the mutual decay of carriers from $|2\rangle$ of the same island to other islands [$\lambda_{ml}^{\mathbf{k}}$ and $\lambda_{ml}^{\prime\mathbf{k}}$ in Eq. (3)], one does not expect that such carrier relaxation processes play significant role in the transport of carriers between the islands. In other words, because the carrier densities in the $|2\rangle$'s of the 19-, 20-, and 21-ML systems are not significantly different and the mean transport time is expected to be long, through these processes each island receives similar number of electrons as it loses. The situation for $\lambda_{l,l+1}^{\prime\prime\mathbf{k}}$ and $\lambda_{l,l-1}^{\prime\prime\mathbf{k}}$, however, is different. These rates mostly represent the net lateral relaxation of electrons from islands associated with fewer ML's to those with more ML's. For the lth ML system they are, respectively, considered here to be equal to $\Gamma_{\mathrm{inter}}\rho_{22}^{l,\mathbf{k}}$ and $\Gamma_{\mathrm{inter}}\rho_{22}^{l-1,\mathbf{k}}$ where $\Gamma_{\mathrm{inter}} = 1/50$ ps^{-1} refers to the rate associated with the mean transport time of electrons from one island to another. Note that obviously such a treatment represents a rough estimate of the effects caused by electron hopping between different islands. In general, these effects depend on scales of the islands and their distributions, carrier densities in each island, temperature, etc. Note also that although the lateral relaxation rate (Γ_{inter}) considered here is at least five times larger than those measured for excitons,[26] it is much smaller than the characteristic damping rates of the upper subbands within one island (Γ_{21} and Γ_{2g}). Therefore, the effect of such a hopping is not very significant if the scale of the islands remains large.

Note that electron-electron interaction influences the intersubband transitions in n-doped QW's via depolarization and exciton effects and renormalization of their conduction subband energies by Hartree and exchange correlations.[34] Although we do not include these issues in this paper, one can speculate their effects considering the fact that here they mainly renormalize the one- and two-photon detunings in Eqs. (4)–(6). One can expect, however, that such an energy renormalization being small[35] and can be incorporated by adjusting the control field detuning. Because of the spatial inhomogeneity of the structure considered in this paper, however, this can only be done for the specific ML system that we want resonant enhancement of refractive index with zero absorption to happen. Under such conditions still different islands have different detunings and are influenced by the control field differently. Therefore, the main concept developed in this paper remains intact.

In the model presented in this paper the signal field is near resonant with the 1-2 transitions. The absorption coefficient and refractive index experienced by this field at different locations of the QW plane (l=19-ML, 20-ML, and 21-ML systems) are found as follows:

$$\alpha^l(\omega_s) = \frac{4\pi\omega_s}{c\mathrm{n_b}}\,\mathrm{Im}[\chi_{21}^l(\omega_s)], \tag{7}$$

$$\mathrm{n}^l(\omega_s) - \mathrm{n_b} = \frac{2\pi}{\mathrm{n_b}}\,\mathrm{Re}[\chi_{21}^l(\omega_s)]. \tag{8}$$

Here n_b is the background refractive index of the QW structure around the 1-2 transition wavelength. $\chi_{21}^l(\omega_s)$ is the sus-

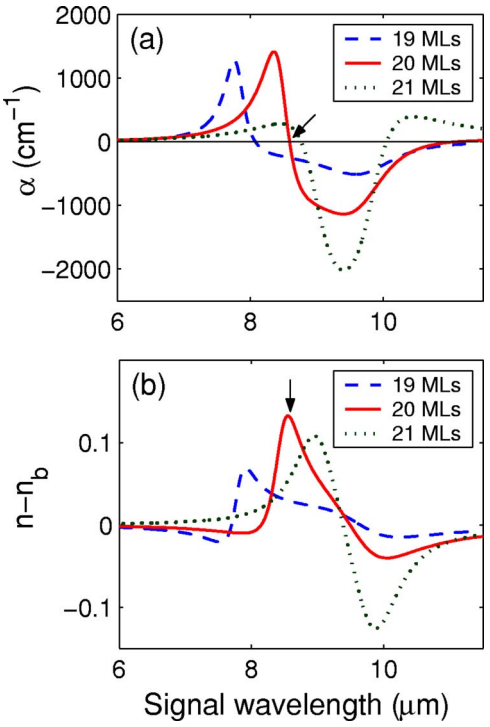

FIG. 4. (Color online) Absorption coefficient (a) and refractive index change (b) of the 1-2 transitions in the 19 (dashed lines), 20 (solid lines), and 21 ML systems (dotted lines). The control field intensity is assumed to be 0.6 MW/cm^2 and its wavelength is 5.59 μm. The arrows refer to λ_s=8.58 μm.

ceptibility of the system for the 1-2 transitions at the lth island given by

$$\chi_{21}^{l}(\omega_s) = \frac{1}{\pi\epsilon L_{\text{eff}}} \frac{\mu_{12}^{l\,2}}{\hbar\Omega_s^l} \int_0^{k_{\max}} k\rho_{12}^{l,k} dk. \tag{9}$$

Here L_{eff} is the effective length over which the 1-2 transitions occur, taken to be the width of the narrower well, and ϵ is the dielectric constant of GaAs at the signal wavelength. $\rho_{12}^{l,k}$ in Eq. (9) was obtained by solving Eqs. (1)–(6) under steady state conditions.

III. AMORPHOUS OPTICAL LATTICES AND RESONANT ENHANCEMENT OF REFRACTIVE INDEX

As pointed out in the preceding section, since the detunings of the control field from the g-2 transitions in different ML systems are not the same the signal field sees these systems differently. To study this issue and discover its physical consequences we start here with the case where the control field intensity (I_c) is 0.6 MW/cm^2 and its wavelength is 5.59 μm. This means that in the lateral regions where the wider well has the nominal thickness (the 20-ML system) the detuning of the control field from the g-2 transitions is about 15 meV. As shown in Fig. 4 (solid lines), under these conditions at the vicinity of 8.58 μm (arrows) the refractive indices of the 1-2 transitions in these regions are enhanced significantly ($n-n_b$=0.13) while their absorption coefficients are diminished. In other words, the so-called resonant enhancement of refractive index with zero absorption occurs.[36] Similar to the atomic systems,[37,38] here the zero absorption occurs at the crossing point of the gain and absorption regions (arrow). Note that when the control field is off (I_c =0) the 1-2 transitions are transparent (zero absorption) and their refractive indices are similar to that of the background of the QW structure, i.e., $n=n_b$.

The enhancement of refractive index with zero absorption seen in Fig. 4 (arrows) is the result of the optimized balance between quantum interference in the intersubband transitions and the incoherent pumping of $|g\rangle$ caused by tunneling of electrons out of $|1\rangle$. The situation is different for the 19-ML and 21-ML systems if we consider that the control field intensity and wavelength remained unchanged, i.e., 0.6 MW/cm^2 and 5.59 μm, respectively. Since in such systems the transition energies are different from those in the 20-ML systems, the control field is detuned from the g-2 transitions by about 30 meV in the 19-ML systems and −1 meV in the 21-ML systems. Here because of the very small or large detuning the quantum coherence and its interplay with the effects caused by the electron tunneling are changed to some extent. As shown in Fig. 4 (dashed lines), the large control field detuning in the 19-ML systems significantly changes their absorption and refractive index spectra compare to those of the 20-ML systems. Despite this still one can see here an enhancement of refractive index with zero absorption. This, however, happens at shorter wavelength with an index augmentation less than half of that seen in the case of the 20-ML system. As shown in Fig. 4 (dotted lines), due to the small detuning of the control field from the g-2 transitions, in the 21-ML systems the electron population in the upper subbands ($|2\rangle$) is relatively higher than those in the 19-ML and 20-ML systems. As a result, the 1-2 transitions here show a significant amount of gain. The resonant enhancement of refractive index with zero absorption here occurs at a longer wavelength and, similar to the 19-ML systems, the refractive index increase is less than that seen in the 20-ML system.

The results presented in Fig. 4 show how various ML systems response differently to a signal field when they are interacting with an identical intense ir laser field. To study the lateral response of the QW and formation of an amorphous two-dimensional optical lattice we need to include the effects of the statistical lateral profiles of the ML growth islands. To do this we assume that the 19-, 20- and 21-ML systems considered in Fig. 2 have the same lateral morphology as that shown in Fig. 3. Under the same conditions as those in Fig. 4 and when the signal field wavelength (λ_s) is 8.58 μm we find the lateral absorption of the QW structure as shown in Fig. 5(a). This figure visualizes the fact that here since the nominal regions (the 20-ML systems) have coherently become transparent ($\alpha^{20\text{-ML}}$=0), the signal field can propagate through this region without any attenuation. On the other hand, because their refractive indices are enhanced more significantly than the other ML systems [Fig. 5(b)], the signal field can also become optically confined in these regions. As shown in Fig. 5(a), under the same conditions, the 19-ML systems generate isles of gain ($\alpha^{19\text{-ML}} \sim -254$ cm^{-1}) with $n-n_b$=0.03 [Fig. 5(b)]. The 21-ML systems, on the

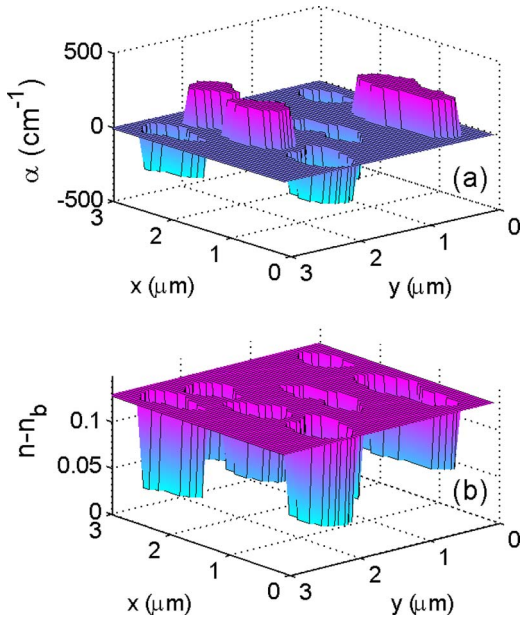

FIG. 5. (Color online) Lateral response of the 19-, 20-, and 21-ML systems with the interface morphology shown in Fig. 3 when the signal field wavelength is 8.58 μm. (a) refers to the absorption coefficient and (b) to the refractive index change in the QW plane. All other specifications are the same as those in Fig. 4.

other hand, create regions of absorption ($\alpha^{21\text{-ML}} \sim 246$ cm^{-1}) with $n-n_b=0.06$.

Note that in the absence of the control field the 8.58 μm signal field propagating along the QW plane only sees a transparent medium with a uniform refractive index equal to n_b. Figure 5 illustrates how this situation changes drastically in the presence of the control laser as various types of coherent mixing of the conduction subbands in different regions of the QW plane form an amorphous optical lattice. Although, morphology of such a lattice is directly influenced by the statistics of the QW interface roughness, it can be optically manipulated by varying the intensity and/or frequency of the control field. In fact by adjusting these parameters one can decide which regions in the QW plane will become transparent with very high refractive indices and which regions will have high absorption or gain with smaller indices. In other words, one can optically control the morphology of the two-dimensional optical lattice to a large extent. This is a significant feature with useful applications as it can establish a ground for active control of light propagation in planar structures. Such a control determines scattering of the light from the coherently generated isles of refractive index, absorption, and gain in the QW plane and determines its attenuation and amplification. This also allows one to change the relative contributions of these islands, causing a dramatic changes in the absorption spectrum of the signal field.

To experimentally realize such an optical lattice one can sandwich the double-QW structure shown in Fig. 2 between two optical confinement layers, forming a waveguide structure similar to those in semiconductor lasers. Note, however, if the number of the double QWs increases the distinct effects discussed in this section are smeared out to some extent. In addition, in the absence of the control field, if the

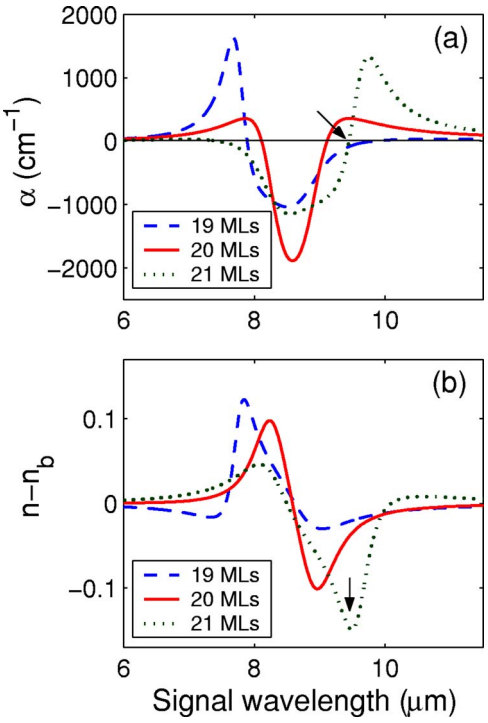

FIG. 6. (Color online) Absorption coefficient (a) and refractive index change (b) of the 1-2 transitions in the 19-ML (dashed lines), 20-ML (solid lines), and 21-ML (dotted lines) systems. The control field intensity is assumed to be 0.6 MW/cm^2 and its wavelength is 5.23 μm. The arrows refer to $\lambda_s=9.45$ μm.

signal field becomes near resonant with the g-2 transitions, it absorption shows some signatures of the growth islands. These include inhomogeneous broadening of the absorption spectra and even the possibility of generation of some kind of ML splitting peaks.[18]

IV. AMORPHOUS OPTICAL LATTICES AND RESONANT SUPPRESSION OF REFRACTIVE INDEX

The coherent processes discussed in the preceding section was optimized to reach large enhancement of refractive index with zero absorption in the conduction intersubband transitions of the 20-ML systems. A distinct feature of the model proposed in this paper is that one can adjust the detuning of the control field to coherently suppress the refractive index of these transitions while making them transparent. To see this, here we employ the same QW system as that considered in Fig. 2 and assume the lateral morphology of the ML islands is the same as that shown in Fig. 3. Here we first consider coherent suppression of refractive indices of the 21-ML systems while their absorption coefficients become zero. Therefore, we consider the wavelength of the control field is 5.23 μm, i.e., it is detuned from the g-2 transitions in these systems by about −16 meV. Under these conditions, as shown in Fig. 6(b) (dotted line), when $I_c=0.6$ MW/cm^2 the refractive indices of the 21-ML systems for $\lambda_s \sim 9.45$ μm (arrow) are coherently suppressed well below the background index ($n-n_b=-0.15$). As seen in Fig. 6(a) (dotted line), around the same wavelength this process is

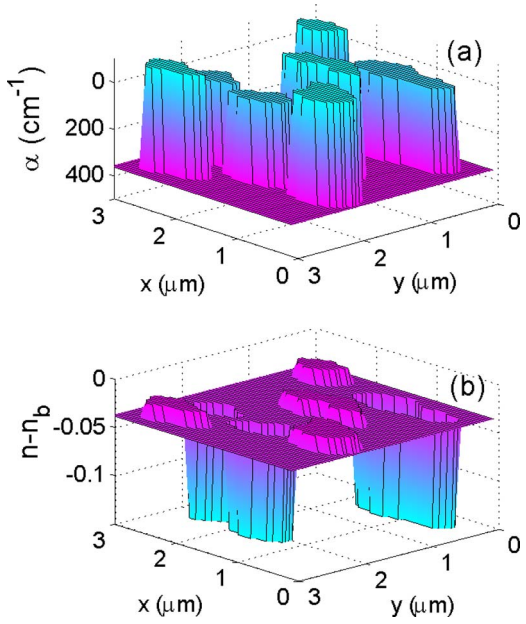

FIG. 7. (Color online) Lateral response of the QW structure shown in Fig. 2 with the interface morphology shown in Fig. 3 when the signal field wavelength is 9.45 μm. (a) refers to the absorption coefficient and (b) to the refractive index change. Other specifications are the same as those in Fig. 6.

accompanied with the reduction of the absorption coefficients of the 1-2 transitions to zero (arrow). Around the same wavelength the 19-ML systems (dashed lines) with control field detuning of about 15 meV show very small amount of absorption without any significant change of refractive index from that of the background. The 20-ML systems (solid lines) here present the resonant case, as the control field in such systems is resonant with the g-2 transitions. As shown in Fig. 6, at λ_s=9.45 μm (arrow) this leads to a slight change of refractive index and generation of some absorption.

To visualize how these processes lead to the lateral modulation of the near resonant responses of the 1-2 transitions in the QW plane and formation of an amorphous optical lattice, here we assume that the control field intensity is 0.6 MW/cm^2 and its wavelength is 5.23 μm, i.e., the same as those in Fig. 6. An oblique three-dimensional illustration of the in-plane response of the QW structure when the signal wavelength is assumed to be 9.45 μm is shown in Fig. 7. Because of the large suppression of refractive index accompanied with zero absorption, Fig. 7(b) shows deep valleys (minima) associated with the 21-ML systems. On the other hand, since the refractive indices of the 19-ML systems are nearly the same as n_b, they form isles of $n-n_b \sim 0$ within the regions with $n-n_b \sim -0.04$ associated with the 20-ML systems. Figure 7(a) shows that the 19-ML and 21-ML systems also form isles of slight gain or nearly zero absorption, respectively, within the highly absorbing regions associated with of the 20-ML systems. (Note that, for the sake of better visualization, here the absorption axis is reversed.) Similar to the previous case, here also one can control the gain and refractive indices of different regions in the QW plane by changing the frequency and/or intensity of the control field.

Figures 6 and 7 present the case where optimization of control field wavelength and intensity led to a dramatic sup-

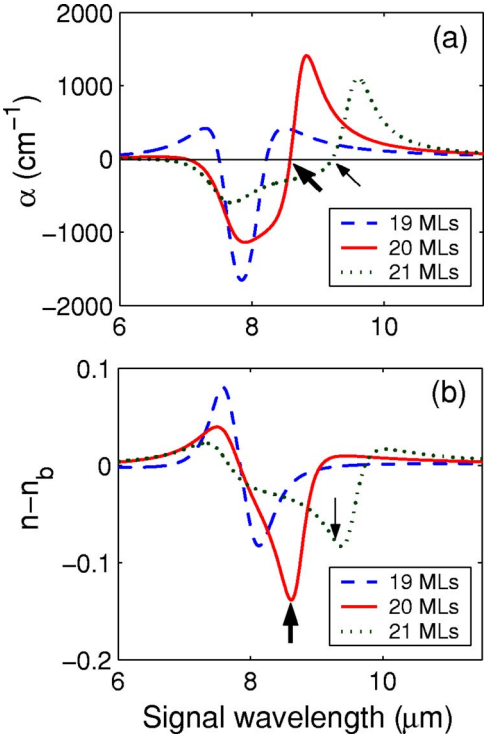

FIG. 8. (Color online) Absorption coefficient (a) and refractive index change (b) of the 1-2 transitions in the 19-ML (dashed lines), 20-ML (solid lines), and 21-ML (dotted lines) systems. The control field intensity is assumed to be 0.6 MW/cm^2 and its wavelength is 4.92 μm. Thick arrows refer to λ_s=8.58 μm and thin arrows to λ_s=9.21 μm.

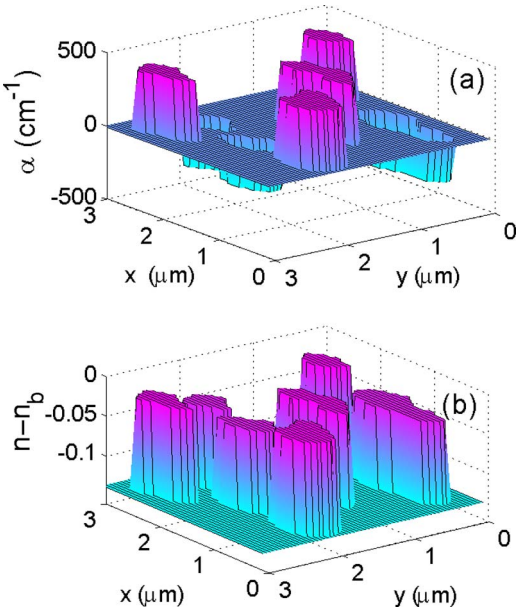

FIG. 9. (Color online) Lateral response of the QW structure shown in Fig. 2 with the interface morphology shown in Fig. 3 when the signal field wavelength is 8.58 μm. (a) refers to the absorption coefficient and (b) to the refractive index change. Other specifications are the same as those in Fig. 8.

pression of the refractive index of the 21-ML systems at a specific wavelength while at the same wavelength the other systems exhibit much smaller index changes. Inspection of this Fig. 6 also shows that under the same conditions in the vicinity of 8 μm one can see coherent enhancement of refractive index accompanied with zero absorption in the 19-ML or 20-ML systems. Around this wavelength, however, the control field does not cause significant refractive index and absorption contrasts between various islands.

The results presented in Fig. 5 illustrated a case where the 20-ML systems became transparent while their refractive indices were enhanced more than those of the 19- and 21-ML systems. This case imitates somehow the case of two-dimensional photonic band gaps formed by putting periodic air cylinders in a semiconductor slab.[39] A complementary case happens when one makes the 20-ML systems transparent while reducing their refractive indices lower than those of other ML systems, i.e., generating an inverted lattice. To inspect this case we show in Fig. 8 the responses of these systems when the wavelength of the control field is adjusted to 4.92 μm and its intensity is kept at 0.6 MW/cm^2. Here at λ_s=8.58 μm the refractive indices of the 20-ML systems are suppressed while they become transparent (thick arrows). The lateral response of the QW at this wavelength shows formation of the inverted amorphous optical lattice where the refractive index contrast between the main 20-ML regions and the 19- and 21-ML systems is about 0.1 [Fig. 9(b)]. Note also that Fig. 8 shows that under the same conditions at a longer wavelength (λ_s=9.21 μm) the resonant suppression of refractive index with zero absorption occurs for the 21-ML systems (thin arrows).

V. CONCLUSIONS

In conclusion, we proposed formation of a quantum-well-based amorphous optical lattice using coherent control of the absorption and refractive index of the intersubband transitions in the plane of an *n*-doped double-QW structure. This was done using the interface morphology of the QW structure and utilizing coherent optical processes in the conduction intersubband transitions. These processes, which were caused by an intense ir field, included resonant suppression or enhancement of refractive indices of these transitions while their absorption coefficients were coherently controlled. We used large-scale ML growth islands at the well/barrier interface to spatially modulate the effects of the intense ir field in the QW plane. The results showed that the intense ir field can convert the QW plane from being a transparent medium with uniform refractive index in the absence of this field into regions with different refractive indices and absorption coefficients. We showed that when the intensity and frequency of this field are chosen properly some of these regions could become transparent with very high or low refractive indices while others acquired a large amount of gain or absorption with different refractive indices. Depending on the morphology of the growth islands, by changing the intense ir field frequency and intensity one can laterally switch over these regions in the QW plane, deciding which locations in this plane become transparent with coherently suppressed or enhanced refractive indices.

ACKNOWLEDGMENTS

I thank Norman Laman for his help in the numerical calculations of this paper.

*Present address: Department of Electrical and Computer Engineering, McMaster University, 1280 Main Street West, Hamilton, Canada, L8S 4K1. Electronic address: sadeghism@ece.mcmaster.ca

[1] A. Andre and M. D. Lukin, Phys. Rev. Lett. **89**, 143602 (2002).
[2] M. Hubner, J. P. Prineas, C. Ell, P. Brick, E. S. Lee, G. Khitrova, H. M. Gibbs, and S. W. Koch, Phys. Rev. Lett. **83**, 2841 (1999).
[3] J. P. Prineas, C. Ell, E. S. Lee, G. Khitrova, H. M. Gibbs, and S. W. Koch, Phys. Rev. B **61**, 13863 (2000).
[4] J. P. Prineas, J. Y. Zhou, J. Kuhl, H. M. Gibbs, G. Khitrova, and S. W. Koch, Appl. Phys. Lett. **81**, 4332 (2002).
[5] S. M. Sadeghi, W. Li, and H. M. van Driel, Phys. Rev. B **69**, 073304 (2004).
[6] I. H. Deutsch, R. J. C. Spreeuw, S. L. Rolston, and W. D. Phillips, Phys. Rev. A **52**, 1394 (1995).
[7] M. Weidemuller, A. Gorlitz, T. W. Hansch, and A. Hemmerich, Phys. Rev. A **58**, 4647 (1998).
[8] S. M. Sadeghi and J. Meyer, Phys. Rev. A **58**, 2534 (1998).
[9] S. M. Sadeghi, H. M. van Driel, and J. M. Fraser, Phys. Rev. B **62**, 15386 (2000).
[10] J. Faist, F. Capasso, C. Sirtori, D. Sivco, J. Baillargeon, A. Hutchinson, S.-N. G. Chu, and A. Cho, Appl. Phys. Lett. **68**, 3680 (1996).
[11] M. A. Herman, D. Bimberg, and J. Christen, J. Appl. Phys. **70**, R1 (1991).
[12] J. Christen, M. Grundmann, and D. Bimberg, J. Vac. Sci. Technol. B **9**, 2358 (1991).
[13] D. Bimberg, J. Christen, T. Fukunaga, H. Nakashima, D. E. Mars, and J. N. Miller, J. Vac. Sci. Technol. B **5**, 1191 (1987).
[14] R. F. Kopf, E. F. Schubert, T. D. Harris, R. S. Becker, and G. H. Gilmer, J. Appl. Phys. **74**, 6139 (1993).
[15] H. Castella and J. W. Wilkins, Phys. Rev. B **58**, 16186 (1998).
[16] S. M. Sadeghi and J. Meyer, Phys. Rev. B **61**, 16841 (2000).
[17] F. T. Vasko, P. Aceituno, and A. Hernandez-Cabrera, Phys. Rev. B **66**, 125303 (2002).
[18] F. T. Vasko, J. P. Sun, G. I. Haddad, and V. V. Mitin, J. Appl. Phys. **87**, 3582 (2000).
[19] O. Gauthier-Lafaye, S. Sauvage, P. Boucaud, F. Julien, F. Glotin, R. Prazeres, J.-M. Ortega, V. Thierry-Mieg, and M. Planel, J. Appl. Phys. **83**, 2920 (1998).
[20] O. Gauthier-Lafaye, B. Seguin-Roa, F. H. Julien, P. Collot, C. Sirtori, J. Y. Duboz, and G. Strasser, Physica E (Amsterdam) **7**, 12 (2000).
[21] F. Grosse and R. Zimmermann, Superlattices Microstruct. **17**, 4399 (1995).
[22] C. Metzer, G. H. Dohler, and H. Sakaki, Phys. Status Solidi A

164, 471 (1997).
[23] D. S. Citrin, Phys. Rev. B **47**, 3832 (1993).
[24] L. Schrottke, H. T. Grahn, and K. Fujiwara, Phys. Rev. B **56**, R15553 (1997).
[25] H. Hillmer, A. Forchel, C. W. Tu, and R. Sauer, Semicond. Sci. Technol. **7**, B235 (1992).
[26] B. Deveaud, T. C. Damen, J. Shah, and C. W. Tu, Appl. Phys. Lett. **51**, 828 (1987).
[27] M. Kohl, D. Heitmann, S. Tarucha, K. Leo, and K. Ploog, Phys. Rev. B **39**, 7736 (1989).
[28] R. Nagarajan, T. Fukushima, S. W. Corzine, and J. Bowers, Appl. Phys. Lett. **59**, 1835 (1991).
[29] S. M. Sadeghi, S. R. Leffler, J. Meyer, and E. Mueller, J. Phys.: Condens. Matter **10**, 2489 (1998).
[30] J. Li and C. Z. Ning, Physica E (Amsterdam) **22**, 628 (2004).
[31] F. Rossi, S. Haas, and T. Kuhn, Phys. Rev. Lett. **72**, 152 (1994).
[32] C. Sirtori, J. Faist, F. Capasso, D. L. Sivco, A. L. Hutchinson, S. N. G. Chu, and A. Y. Cho, Appl. Phys. Lett. **68**, 1745 (1996).
[33] J. Wang, J.-P. Leburton, Z. Moussa, F. H. Julien, and A. Saar, J. Appl. Phys. **80**, 1970 (1996).
[34] S. L. Chuang, M. S. C. Luo, S. Schmitt-Rink, and A. Pinczuk, Phys. Rev. B **46**, 1897 (1992).
[35] D. J. Newson and A. Kurobe, Appl. Phys. Lett. **51**, 1670 (1987).
[36] M. O. Scully and M. S. Zubiary, *Quantum Optics* (Cambridge University Press, Cambridge, England, 1997).
[37] U. Rathe, M. Fleischhauer, S.-Y. Zhu, T. W. Hansch, and M. O. Scully, Phys. Rev. A **47**, 4994 (1993).
[38] A. S. Zibrov, M. D. Lukin, L. Hollberg, D. E. Nikonov, M. O. Scully, H. G. Robinson, and V. L. Velichansky, Phys. Rev. Lett. **76**, 3935 (1996).
[39] U. Gruning, V. Lehmann, S. Ottow, and K. Busch, Appl. Phys. Lett. **68**, 747 (1996).